ACS OMEGA

http://pubs.acs.org/journal/acsodf

Article

Preparation of Biomass-Based Carbon Dots with Aggregation Luminescence Enhancement from Hydrogenated Rosin for Biological Imaging and Detection of Fe^{3+}

Jundan Zhou, Min Ge, Youqi Han, Jiaxin Ni, Xun Huang, Shiyan Han,* Zhibin Peng, Yudong Li, and Shujun Li*

Cite This: *ACS Omega* 2020, 5, 11842−11848

Read Online

ACCESS | Metrics & More | Article Recommendations | Supporting Information

ABSTRACT: Fluorescent carbon dots (CDs) have numerous important applications, but enhancing the fluorescence emission and overcoming fluorescence quenching are still big challenges. Here, fluorescence-enhanced carbon dots (named hr-CDs) were prepared from sustainable hydrogenated rosin, using a simple hydrothermal method in a water solvent. The hr-CDs were mainly composed of graphitized carbon cores with surface functional groups. With the increase in the concentration to hr-CDs aqueous solutions, the distance between the carbon cores decreased, which resulted in the formation of J aggregates and the enhanced blue fluorescence emission. Even in the solid state, the hr-CDs show fluorescence emission because the surface functional groups could prevent $\pi-\pi$ stacking interactions between the carbon cores. The hr-CDs show excellent resistance to photobleaching under intense ultraviolet light (200 mW/cm^2). Vibrations and rotations of graphitized carbon core are restricted by low temperature and high viscosity, leading to increased radiative transition and thus increase in fluorescence intensity. The pH value in the range of 3.99−9.87 and anions have little effect on the fluorescence emission of hr-CDs. The fluorescence emission of the hr-CDs was selectively quenched by Fe^{3+} and can thus be used to detect Fe^{3+}. The hr-CDs also have good biocompatibility and show the same ability in cell nuclear staining as 4′,6-diamidino-2-phenylindole (DAPI).

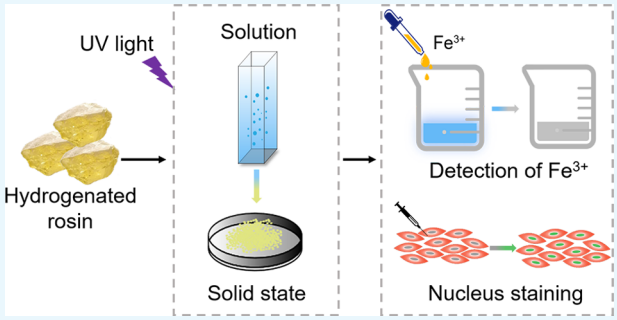

INTRODUCTION

There have recently been numerous peer-reviewed articles that describe carbon dots (CDs) with excellent optical properties and discuss their potential as substitutes for conventional fluorescent materials, such as fluorescent organic dyes and inorganic fluorescent nanoparticles.[1−4] Because of their many advantages, including tunable fluorescence, low toxicity, good biocompatibility, and resistance to photobleaching,[5−11] CDs has been widely used as biomarkers, photocatalysts, and white light emitting diodes (WLEDs).[8,12−16] Many kinds of raw materials, which can be broadly classified as either organic materials derived from industrial synthesis[17,18] or naturally occurring biomass materials,[19] have been successfully converted into CDs using increasingly sophisticated synthetic methods.[20,21] Simple and economical methods for converting low-cost renewable biomass materials into CDs, especially, have received much attention recently. A wide variety of renewable biomass materials, including corn,[21] starch,[22] enokitake mushrooms,[23] various fruits,[24−26] rice husks,[27,28] chitosan,[29] alkali lignin,[30] and willow catkins[31] have now been used to prepare CDs. Taking every factor into account, however, current methods for producing CDs all have shortcomings. In many regions of the world, food is in short supply and it is wasteful to use edible materials to prepare CDs. Reported technologies to synthesize CDs also usually require high-temperature calcination, strong acid or strong alkali for deep carbonization,[32] or extraction with organic solvents,[33] which require massive consumption of energy and materials. Another drawback is that the fluorescence of many CDs is quenched in more concentrated solutions. Some CDs totally lose their fluorescence in the solid state by a process known as aggregation-caused quenching (ACQ), which is caused by fluorescence resonance energy transfer and direct $\pi-\pi$ interactions.[34] ACQ remains the Achilles heel that restricts the wider application of CDs. Some CDs, however, show aggregation-induced emission enhancement (AIEE) instead and avoid fluorescence attenuation by radiative recombination.[35,36] There is currently a real need for novel CDs with

Received: April 4, 2020
Accepted: April 30, 2020
Published: May 12, 2020

https://dx.doi.org/10.1021/acsomega.0c01527
ACS Omega 2020, 5, 11842−11848

AIEE. Here, we report a new type of CDs, named hr-CDs, which can be prepared from hydrogenated rosin, a biomass raw material with a unique ternary ring structure, by a one-step hydrothermal method in an aqueous solvent environment, without the need for a dopant or purification, and also avoid the introduction of toxic reagents through a method that is different from the one reported. The preparation of hr-CDs is shown in Scheme 1. The prepared hr-CDs solution emits a

Scheme 1. Schematic Illustration Showing Preparation of Fluorescence Enhancement Carbon Dots from Hydrogenated Rosin

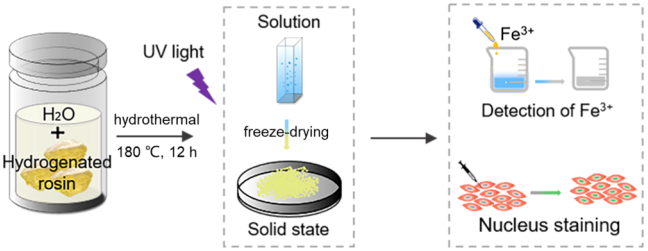

blue fluorescence with an enhanced intensity as the concentration is increased. Even in the solid state, the hr-CDs, which have a yellow-green emission, are different from the conventional carbon dots with aggregation fluorescence quenching in the solid state.[37] The hr-CDs can be used not only as a fluorescent probe for detecting Fe^{3+} but also for cell imaging.

RESULTS AND DISCUSSION

Characterization of hr-CDs. The as-prepared hr-CDs were dissolved in deionized water and their morphology was investigated by transmission electron microscopy (TEM). The carbon dots possessed a spherical appearance (Figure 1a), with an average diameter of 1.5 nm (Figure S1). The lattice fringes of the hr-CDs display interplanar spacings of 0.21 and 0.24 nm (Figure 1a, inset), which correspond to the (100)[38] plane of graphitic carbon and the (1120)[39,40] lattice fringes of graphene, respectively. In the UV−vis spectra (Figure 1b), compared with hydrogenated rosin, the hr-CDs showed significantly enhanced absorption over the range 247−320 nm due to the absorption bands of $\pi-\pi^*$ and $n-\pi^*$ transitions.[18,41] Since the spectra of hydrogenated rosin and hr-CDs were determined at the same concentration, this indicates a more conjugated structure in the hr-CDs, compared with hydrogenated rosin. X-ray diffraction analysis showed that the diffraction peak position of the graphite carbon cores is noticeably influenced by the structure of the raw material (Figure S2). The Fourier transform infrared (FTIR) spectrum of the hr-CDs (Figure 1c) showed that peaks were consistent with hydrogenated rosin. Proton nuclear magnetic resonance (^{1}H NMR) spectra (Figure 1d) were used to determine the structure of the hr-CDs. Aromatic H signals seen in the range of 6.0−8.0 ppm may be attributed to graphitized carbon core proton resonance.[35,42] Analysis of the hr-CDs by high-resolution X-ray photoelectron spectroscopy (XPS) of C 1s (Figure 1e) and O 1s (Figure 1f) indicated the presence of C−C/C═C, C═O, C−O, and O−C═O groups.[43−45] The above results proved the existence of the basic structural−functional group unit molecule of hydrogenated rosin on the surface of the carbon core.

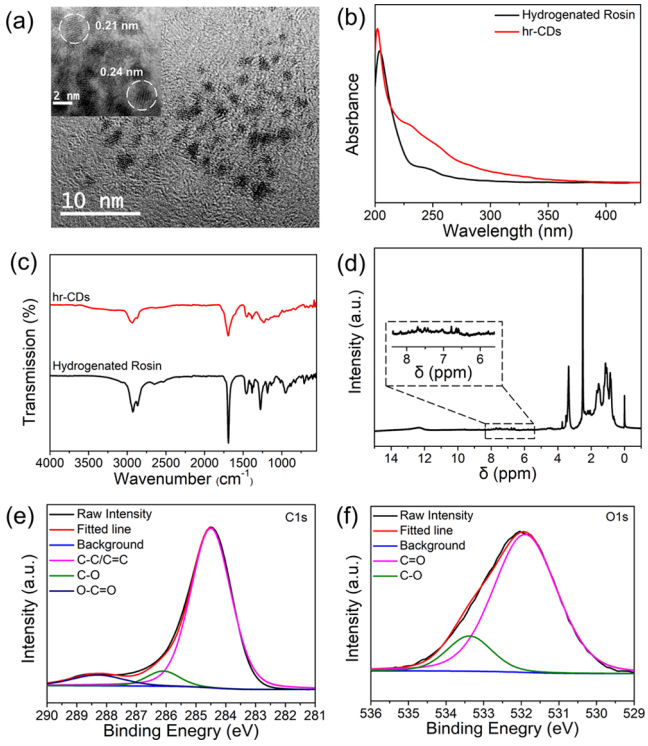

Figure 1. (a) TEM image of hr-CDs (inset: high-resolution TEM (HR-TEM)). (b) UV−vis spectra of solutions of hydrogenated rosin (10 μg/mL) and hr-CDs (10 μg/mL). (c) FTIR spectra of hr-CDs and hydrogenated rosin. (d) ^{1}H NMR spectra of hr-CDs. High-resolution XPS C 1s (e) and O 1s (f) of hr-CDs.

Photoluminescence (PL) Properties of hr-CDs. To determine the potential of hr-CDs in bioimaging, we first investigated their fluorescence properties. An aqueous solution of hr-CDs is blue (Figure 2a inset) under 365 nm UV light and the fluorescence emission spectrum of the aqueous solution was shown to be excitation dependent (Figure 2a). The fluorescence intensity reached a maximum when the excitation wavelength was 310 nm, with the strongest emission peak at 442 nm (Figure 2a). Fluorescence emission spectra of aqueous solutions of hr-CDs with different concentrations (Figure 2b) showed a stable enhancement from 1.0 to 20.0 μg/mL. This may be attributable to the formation of J-aggregate-like structures between graphite carbon cores when the concentration of hr-CDs is increased.[35] The fluorescence lifetime of hr-CDs in a solution was 2.16 ns (Figure S3), with a PL quantum yield of 1.22%. Notably, the solid powder showed a strong fluorescence emission peak at 550 nm with excitation at 480 nm and yellow-green fluorescence under ultraviolet irradiation (365 nm) (Figure 2c, inset). The research has shown that the yellow-green fluorescence emitting carbon dots worked as a color conversion layer to fabricate white light emitting diode (WLED)[38] so the prepared hr-CDs could be potentiality used to fabricate WLED. The solid-state fluorescence emission was also found to be excitation dependent (Figure 2c), mainly because the functional group on the surface of carbon cores effectively prevents $\pi-\pi$ stacking interactions, thus contributing to the solid-state emission fluorescence.[38] The resistance of the hr-CDs to photobleaching was investigated using commercially available 4′,6-diamidino-2-phenylindole (DAPI) as the control. Upon irradiation with UV light, the fluorescence of the hr-CDs

https://dx.doi.org/10.1021/acsomega.0c01527
ACS Omega 2020, 5, 11842−11848

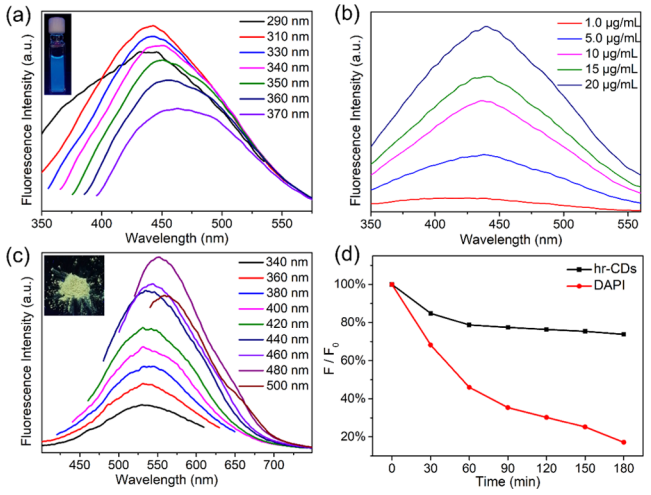

Figure 2. (a) Fluorescence spectra of an aqueous solution of hr-CDs (20 μg/mL) at different excitation wavelengths (inset: photograph showing the fluorescence of aqueous solution of hr-CDs under 365 nm ultraviolet irradiation). (b) Fluorescence spectra of the aqueous solutions of hr-CDs with different concentrations (Ex = 310 nm). (c) Fluorescence spectra of solid hr-CDs (inset: photograph showing fluorescence of solid hr-CDs under 365 nm ultraviolet irradiation). (d) Fluorescence intensity of aqueous solution of hr-CDs (10 μg/mL) and DAPI (10 μg/mL) after irradiation with UV lamp (200 mW/cm^2) for different periods of time.

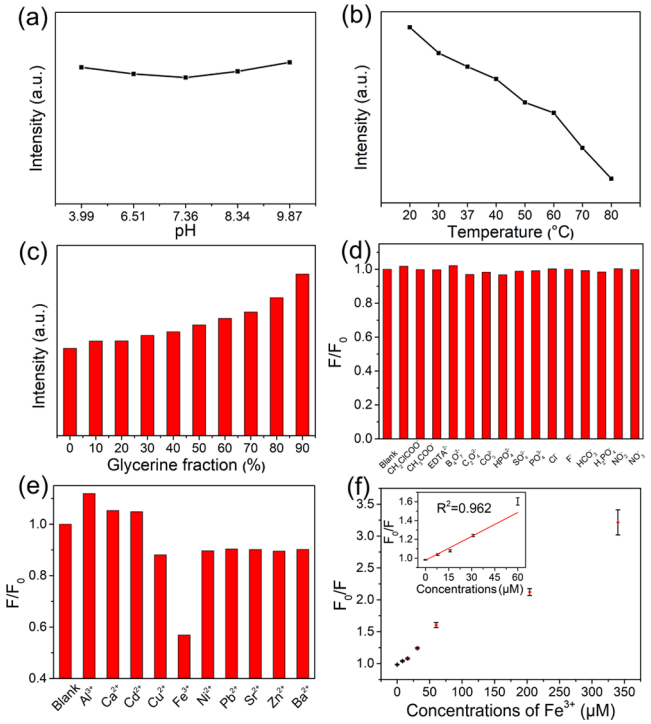

Figure 3. (a) Changes in the fluorescence intensity of the aqueous solutions of hr-CDs (10 μg/mL) at different pH values. (b) Changes in the fluorescence intensity of aqueous solutions of hr-CDs (20 μg/mL) at different temperatures. (c) Changes in the fluorescence intensity of solutions of hr-CDs (20 μg/mL) in different mixtures of water and glycerol. (d, e) Fluorescence intensity ratio of an aqueous solution of hr-CDs (20 μg/mL) on the addition of different ions (F_0 and F are fluorescence intensities without and with ions, respectively). (f) Dependence of F_0/F on the concentration of Fe^{3+} ions over the range 0−340 μM (inset: linear relationship of F_0/F versus the concentration of Fe^{3+} ions over the concentration range 0−60 μM).

decreased by ∼25% in the first 60 min and then remained stable (Figures 2d and S4). The fluorescence intensity of DAPI, on the other hand, continued to decrease after 60 min, with a total reduction of ∼80% after 180 min (Figure 2d). It is worth noting that the UV irradiance that we use is 200 mW/cm^2, which is 2000-fold higher than the intensity used in a recently reported study.[45]

The fluorescence intensity of carbon dots is influenced by factors such as pH, temperature, metal ions, and some anions. To better understand the potential applications of hr-CDs, we next investigated the effect of pH on fluorescence intensity. The fluorescence intensity of the hr-CDs was stable, with little obvious changes, over the pH range of 3.99−9.87 (Figures 3a and S5). This is the pH range of intracellular microenvironments,[46] suggesting that the hr-CDs are suitable for cellular imaging. The fluorescence intensity of an aqueous solution of hr-CDs decreased as the temperature increased (Figures 3b and S6). Since vibration and rotation of graphitized carbon core with functional groups are restricted at lower temperatures, there is increased radiative transition and thus increased fluorescence intensity.[45] The effect of viscosity on the fluorescence intensity of hr-CDs was investigated using different proportions of water and glycerin as the solvent. The fluorescence intensity increased with increasing amounts of glycerin (Figures 3c and S7) because the higher viscosity inhibits the vibration and rotation of the carbon dots, thus increasing the radiative transitions.

Selectivity and Sensitivity of hr-CDs. The experiment was carried out to test the fluorescent response of the hr-CDs to various anions (Figures 3d and S8) and cations (Figures 3e and S9) by adding the test ion (50 μM) to an aqueous solution of hr-CDs (20 μg/mL). F_0 is the fluorescence intensity of the solution of hr-CDs without added ions and F is the intensity of the solution with added ions. A wide variety of anions had very little effect on the fluorescence intensity (Figures 3d and S8). Cations, on the other hand, had different individual effects on the fluorescence intensity (Figures 3e and S9). The most obvious quenching was caused by Fe^{3+} (Figure 3e), likely because the open d orbitals of Fe^{3+} can coordinate easily with the hydroxyl groups.[28] When Fe^{3+} binds to the hr-CDs, which act as electron donors, the d orbitals of the Fe^{3+} split. Some electrons in the excited state are then transferred from the hr-CDs to the d orbitals of Fe^{3+},[30] reducing the proportion of radiative transition and leading to fluorescence quenching.[45] Then, we explored the feasibility of using hr-CDs for the detection of Fe^{3+} (Figure S10). On the addition of Fe^{3+}, there was a marked decrease in fluorescence intensity, and in the range of 0−60 μM, the Fe^{3+} concentration fits well with the fluorescence intensity ratio (F_0/F) by linear equation (Figure 3f) and the equation is $F_0/F = 0.00845C + 0.9781$, where the C is the concentration of Fe^{3+}. The detection limit was about 6.16 μM, which was lower than that reported by the previous Fe^{3+} detection systems based on CDs.[47,48]

Cytotoxicity and Cell Imaging of hr-CDs. For years, CDs have been reported to achieve outstanding imaging quality in cell biology. To demonstrate the potential of hr-CDs to replace the previously described CDs, we investigated the inherent cytotoxicity and biocompatibility of hr-CDs in MG-63 and human umbilical vein endothelial cells (HUVECs) using standard cell counting kit-8 (CCK-8) assays. The hr-CDs showed excellent biocompatibility with MG-63 (Figure 4a)

https://dx.doi.org/10.1021/acsomega.0c01527
ACS Omega 2020, 5, 11842−11848

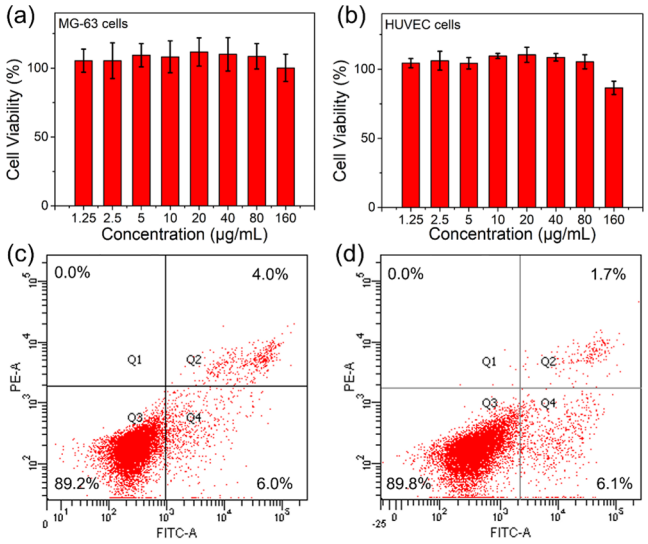

Figure 4. (a, b) Relative viability of MG-63 and HUVECs incubated with a series of gradient concentrations of hr-CDs for 24 h. Cytotoxicity was evaluated by flow cytometry using (c) MG-63 cells and (d) HUVECs treated with hr-CDs (50 μg/mL) for 72 h.

and HUVECs (Figure 4b). Flow cytometry was used to assess cell apoptosis in MG-63 and HUVECs treated with hr-CDs (50 μg/mL) for 72 h. The percentages of apoptotic (Q2 + Q4) MG-63 cells and HUVECs were 10% (Figure 4c) and 7.8% (Figure 4d), respectively, which are no higher than that for normal cell apoptosis (10%).

The hr-CDs were next investigated as a biological dye and incubated with MG-63 and HUVECs for 10 h in a bioimaging study. Images of MG-63 and HUVECs stained with DAPI, which produces a blue color under UV light, are shown in Figure 5a-I,b-I. The images showing a green color under blue light (Figure 5a-II,b-II) are those stained with hr-CDs. DAPI is commonly used as a cell nuclear stain and the images stained by DAPI and hr-CDs overlapped well (Figure 5a-III,b-III), demonstrating that the hr-CDs are also an effective cell nuclear stain.

CONCLUSIONS

Hydrogenated rosin was used as the raw material to synthesize hr-CDs using a simple hydrothermal method. Upon irradiation with 365 nm light, an aqueous solution of hr-CDs and solid hr-CDs emitted blue and yellow-green fluorescence, respectively. Importantly, the hr-CDs had excellent resistance to photobleaching when irradiated with ultraviolet light (200 mW/cm^2), which is 2000-fold higher than the intensity used in a recent report. The hr-CDs could also be used to detect Fe^{3+}, with a detection limit of 6.16 μM. Because of their inherent biocompatibility and low cytotoxicity, the hr-CDs could be used as a cell nuclear stain that is as effective as the commonly used cell nuclear stain, DAPI.

EXPERIMENTAL SECTION

Materials. Hydrogenated rosin (acid value, 170.7 mg KOH/g, specific information is recorded in Table S1) was purchased from Guangxi Hualin Chemical Co., Ltd., China, and DAPI was purchased from Shanghai McLean Biochemical Reagents Co., Ltd., China. $Al(NO_3)_3{\cdot}9H_2O$, $Ca(NO_3)_2{\cdot}4H_2O$, $Cd(NO_3)_2{\cdot}4H_2O$, $Cu(NO_3)_2{\cdot}3H_2O$, and $Fe(NO_3)_3{\cdot}9H_2O$ were purchased from Tianjin Bodi Chemical Industry Co., Ltd., China. $Ni(NO_3)_2{\cdot}6H_2O$, $Pb(NO_3)_2$, $Sr(NO_3)_2$, $Zn(NO_3)_2{\cdot}6H_2O$, $Ba(NO_3)_2$, $CH_3ClCOONa$, CH_3COONa, glycerol, and $NaNO_2$ were purchased from Tianjin Fuyu Fine Chemical Co., Ltd., China. EDTA-2Na, $B_4O_7Na_2$, $C_2O_4Na_2$, Na_2CO_3, Na_2HPO_4, Na_3PO_4, NaCl, NaF, $NaHCO_3$, and NaH_2PO_4 were purchased from Tianjin Yongda Chemical Reagent Co., Ltd., China. All reagents were analytical grade and used as received without further purification. Deionized water was prepared using a Clever-Q30 UT water filtration system Zhiang Instrument Co., Ltd. (Shanghai, China). A cell counting kit-8 (CCK-8) assay kit was purchased from Dojindo Laboratories (Kumamoto, Japan), and Normocin was purchased from InvivoGen (San Diego). Fetal bovine serum (FBS), Dulbecco's modified Eagle's medium/Ham's F12 medium (DMEM/F12), and phosphate-buffered saline (PBS) solution were purchased from Gibco and Thermo Fisher Scientific Inc. (Waltham). MG-63 cells and HUVECs

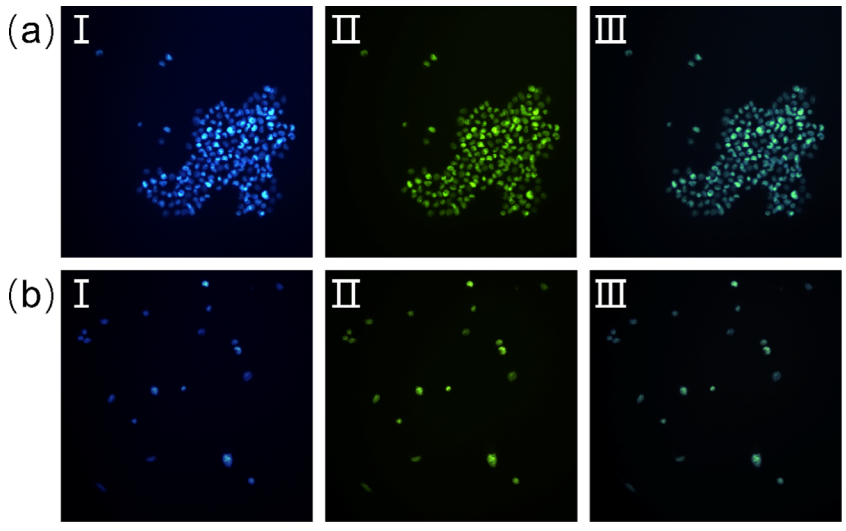

Figure 5. Fluorescence images of (a) MG-63 cells and (b) HUVECs stained by DAPI and incubated with hr-CDs for 10 h. Imaging stained by DAPI in nucleus (I), imaging stained by hr-CDs in nucleus (II), and overlays of the previous two (III).

https://dx.doi.org/10.1021/acsomega.0c01527
ACS Omega 2020, 5, 11842−11848

were purchased from the Chinese Academy of Sciences (Shanghai, China).

Characterization. Transmission electron microscopy (TEM) and high-resolution transmission electron microscopy (HR-TEM) images were collected using a JEM-2100 transmission electron microscope (JEOL, Ltd., Tokyo, Japan). Proton nuclear magnetic resonance (^{1}H NMR) spectra were measured in dimethyl sulfoxide (DMSO) using an AVANCE III HD 500 MHz spectrometer (BrukerCorp, Karlsruhe, Germany). X-ray photoelectron spectroscopy (XPS) was carried out using an Escalab 250Xi X-ray photoelectron spectrometer (Thermo Fisher Scientific Co., Ltd., Shanghai, China). The FTIR spectra were collected using a frontier Fourier transform infrared spectrometer (PerkinElmer Co., Ltd., Waltham, MA). The UV−vis absorption spectra were recorded using a TU-1950 ultraviolet−visible spectrofluorometer (Persee General Instrument Co., Ltd., Beijing, China). Photoluminescence (PL) measurements were carried out using an LS55 fluorescence spectrometer (PerkinElmer Co., Ltd.). Fluorescence decay curves were measured using a DeltaFlex modular fluorescence lifetime instrument (Horiba Jobin Yvon IBH Ltd., Glasgow, U.K.). PL quantum yields were measured using an FLS1000 fluorescence spectrometer (Edinburgh Instruments, Ltd., Edinburgh, U.K.). Fluorescence images were captured using a DMI4000 B inverted fluorescence microscope (Leica Microsystems Inc., Wetzlar, Germany).

Synthesis of hr-CDs. Hydrogenated rosin (0.7 g) was ground to a powder and placed in a 100 mL Teflon-lined stainless autoclave together with deionized water (70 mL). The mixture was heated to 180 °C for 12 h and then allowed to cool to room temperature. The resulting solution was filtered through a 0.22 μm ultrafiltration membrane and then freeze-dried to provide the hr-CDs.

Cytotoxicity Test. The effects of different concentrations of hr-CDs on the viability of HUVECs and MG-63 were determined using a cell counting kit-8 (CCK-8) assay. Cell suspensions, harvested at the exponential growth phase of the cells, were plated onto a 96-well plate at a density of 5000 cells/well. The cells were then grown overnight at 37 °C in a culture medium (10% FBS + 90% DMEM/F12 + 100 μg/mL Normocin) in a humidified atmosphere of 5% CO_2 to ensure that the cells adhered to the orifice plates. The wells were then divided into a blank control group (medium only), a negative control group (medium + cells), and eight test groups (medium + cells + hr-CDs), with eight wells in each group. In the test groups, the cells were cultured in the presence of different concentrations (1.25, 2.5, 5.0, 10, 20, 40, 80, 160 μg/mL) of hr-CDs. The cells were placed in an incubator at 37 °C in a humidified atmosphere of 5% CO_2 for 24 h. CCK-8 (10 μL) was then added to each well, and the cells were incubated for a further 4 h at 37 °C. The absorbance of each well (OD) was measured at 450 nm using a Multiskan GO microplate reader (Thermo Fisher Scientific, Vantaa, Finland). Cell viability was defined as the ratio of absorbance in the presence of hr-CDs to that in the absence of hr-CDs.

$$\text{cell viability (\%)} = (\text{OD}_{\text{test}} - \text{OD}_{\text{bland control}}) / (\text{OD}_{\text{negative control}} - \text{OD}_{\text{bland control}}) \times 100\%$$

Cellular Imaging. HUVECs and MG-63 were inoculated into 48-well plates (10 000 cells/well) with clean cover glass and cultured at 37 °C in a humidified atmosphere of 5% CO_2 for 24 h. Culture medium (10% FBS + 90% DMEM/F12 + 100 μg/mL Normocin) was added, and the cells were cultured with hr-CDs in a saturated humidity incubator at 37 °C under an atmosphere of 5% CO_2 for 10 h. The cover glass was removed and washed three times with PBS. The cells were immobilized with a precooled 4% paraformaldehyde solution for 30 min and then dyed using a solution of DAPI in PBS (10 μg/mL) for 5 min. After each operation, the cover glass was washed three times with PBS. The cover glass was sealed with antifluorescence quenching agent and images were captured using an inverted fluorescence microscope.

■ ASSOCIATED CONTENT

Supporting Information

The Supporting Information is available free of charge at https://pubs.acs.org/doi/10.1021/acsomega.0c01527.

Size distribution histograms of hr-CDs; XRD of hr-CDs and hydrogenated rosin; FL decay spectrum and fitted curves of hr-CDs solutions; fluorescence spectra and fluorescence intensity of aqueous solution of hr-CDs (10 μg/mL) after irradiation with a UV lamp (200 mW/cm^2) for different periods of time; fluorescence spectra of aqueous solutions of hr-CDs (10 μg/mL) at different pH values; fluorescence spectra of aqueous solutions of hr-CDs (20 μg/mL) at different temperatures; fluorescence spectra of solutions of hr-CDs (20 μg/mL) in different mixtures of water and glycerol; fluorescence spectra of an aqueous solution of hr-CDs (20 μg/mL) on the addition of different anions; fluorescence spectra of an aqueous solution of hr-CDs (20 μg/mL) on the addition of different cations; fluorescence spectra of an aqueous solution of hr-CDs (20 μg/mL) in the presence of different concentrations of Fe^{3+} (PDF)

■ AUTHOR INFORMATION

Corresponding Authors

Shiyan Han − *Key Laboratory of Bio-based Material Science and Technology, Ministry of Education, Northeast Forestry University, Harbin 150040, China;* orcid.org/0000-0003-3999-6450; Email: hanshiyan80@163.com

Shujun Li − *Key Laboratory of Bio-based Material Science and Technology, Ministry of Education, Northeast Forestry University, Harbin 150040, China;* orcid.org/0000-0002-3836-5350; Email: lishujun@nefu.edu.cn

Authors

Jundan Zhou − *Key Laboratory of Bio-based Material Science and Technology, Ministry of Education, Northeast Forestry University, Harbin 150040, China*

Min Ge − *Key Laboratory of Bio-based Material Science and Technology, Ministry of Education, Northeast Forestry University, Harbin 150040, China*

Youqi Han − *Key Laboratory of Bio-based Material Science and Technology, Ministry of Education, Northeast Forestry University, Harbin 150040, China*

Jiaxin Ni − *Key Laboratory of Bio-based Material Science and Technology, Ministry of Education, Northeast Forestry University, Harbin 150040, China*

Xun Huang − *Key Laboratory of Bio-based Material Science and Technology, Ministry of Education, Northeast Forestry University, Harbin 150040, China*

https://dx.doi.org/10.1021/acsomega.0c01527
ACS Omega 2020, 5, 11842−11848

Zhibin Peng − *Department of Orthopaedic Surgery, The First Affiliated Hospital of Harbin Medical University, Harbin 150040, China*

Yudong Li − *Key Laboratory of Bio-based Material Science and Technology, Ministry of Education, Northeast Forestry University, Harbin 150040, China*

Complete contact information is available at: https://pubs.acs.org/10.1021/acsomega.0c01527

Author Contributions

J.Z. and M.G. contributed equally to this work. S.H. conceived the idea and supervised the material synthesis and data collection for the paper. M.G. and J.Z. conducted the synthesis experiments. Z.P. conducted the cytotoxicity and cell imaging experiments. Y.H., J.N., and X.H. prepared the figures of the manuscript. S.H. and S.L. discussed the photoluminescence mechanism of hr-CDs. J.Z. wrote the first draft of the manuscript. S.H., Y.L., and S.L. made substantial revisions. All authors read and approved the final manuscript.

Notes

The authors declare no competing financial interest.

■ ACKNOWLEDGMENTS

This work was supported by the National Natural Science Foundation of China (31700502) and the Fundamental Research Funds for the Central Universities (2572017CB17). The authors are grateful for the funding.

■ REFERENCES

(1) Zhang, H.; Zheng, X.; Xie, N.; He, Z.; Liu, J.; Leung, N. L. C.; Niu, Y.; Huang, X.; Wong, K. S.; Kwok, R. T. K.; Sung, H. H. Y.; Williams, I. D.; Qin, A.; Lam, J. W. Y.; Tang, B. Z. Why do simple molecules with "isolated" phenyl rings emit visible light? *J. Am. Chem. Soc.* **2017**, *139*, 16264−16272.

(2) Seike, M.; Nagata, K.; Ikeda, H.; Ito, A.; Sakuda, E.; Kitamura, N.; Shinohara, A.; Yoshimura, T. Synthesis and photoluminescence of tetracyanidonitridorhenium(V) complexes with five-membered N-heteroaromatic ligands and photoluminescence-intensity change. *ACS Omega* **2019**, *4*, 21251−21259.

(3) Asano, H.; Tsukuda, S.; Kita, M.; Fujimoto, S.; Omata, T. Colloidal Zn(Te,Se)/ZnS core/shell quantum dots exhibiting narrow-band and green photoluminescence. *ACS Omega* **2018**, *3*, 6703−6709.

(4) George, N. C.; Brgoch, J.; Pell, A. J.; Cozzan, C.; Jaffe, A.; Dantelle, G.; Llobet, A.; Pintacuda, G.; Seshadri, R.; Chmelka, B. F. Correlating local compositions and structures with the macroscopic optical properties of Ce^{3+}-doped $CaSc_2O_4$, an efficient green-emitting phosphor. *Chem. Mater.* **2017**, *29*, 3538−3546.

(5) Rigodanza, F.; Dordevic, L.; Arcudi, F.; Prato, M. Customizing the electrochemical properties of carbon nanodots by using quinones in bottom-up synthesis. *Angew. Chem., Int. Ed.* **2018**, *57*, 5062−5067.

(6) Atchudan, R.; Edison, T.; Lee, Y. R. Nitrogen-doped carbon dots originating from unripe peach for fluorescent bioimaging and electrocatalytic oxygen reduction reaction. *J. Colloid Interface Sci.* **2016**, *482*, 8−18.

(7) Ensafi, A. A.; Hghighat Sefat, S.; Kazemifard, N.; Rezaei, B.; Moradi, F. A novel one-step and green synthesis of highly fluorescent carbon dots from saffron for cell imaging and sensing of prilocaine. *Sens. Actuators, B* **2017**, *253*, 451−460.

(8) Konar, S.; Kumar, B. N. P.; Mahto, M. K.; Samanta, D.; Shaik, M. A. S.; Shaw, M.; Mandal, M.; Pathak, A. N-doped carbon dot as fluorescent probe for detection of cysteamine and multicolor cell imaging. *Sens. Actuators, B* **2019**, *286*, 77−85.

(9) Choi, Y.; Thongsai, N.; Chae, A.; Jo, S.; Kang, E. B.; Paoprasert, P.; Park, S. Y.; In, I. Microwave-assisted synthesis of luminescent and biocompatible lysine-based carbon quantum dots. *J. Ind. Eng. Chem.* **2017**, *47*, 329−335.

(10) Das, P.; Ganguly, S.; Maity, P. P.; Srivastava, H. K.; Bose, M.; Dhara, S.; Bandyopadhyay, S.; Das, A. K.; Banerjee, S.; Das, N. C. Converting waste allium sativum peel to nitrogen and sulphur co-doped photoluminescence carbon dots for solar conversion, cell labeling, and photobleaching diligences: a path from discarded waste to value-added products. *J. Photochem. Photobiol., B* **2019**, *197*, No. 111545.

(11) Hess, S. C.; Permatasari, F. A.; Fukazawa, H.; Schneider, E. M.; Balgis, R.; Ogi, T.; Okuyama, K.; Stark, W. J. Direct synthesis of carbon quantum dots in aqueous polymer solution: one-pot reaction and preparation of transparent UV-blocking films. *J. Mater. Chem. A* **2017**, *5*, 5187−5194.

(12) Demir, B.; Lemberger, M. M.; Panagiotopoulou, M.; Rangel, P. X. M.; Timur, S.; Hirsch, T.; Bui, B. T. S.; Wegener, J.; Haupt, K. Tracking hyaluronan: molecularly imprinted polymer coated carbon dots for cancer cell targeting and imaging. *ACS Appl. Mater. Interfaces* **2018**, *10*, 3305−3313.

(13) Patra, A. S.; Gogoi, G.; Qureshi, M. Ordered−disordered $BaZrO_{3-\delta}$ hollow nanosphere/carbon dot hybrid nanocomposite: a new visible-light-driven efficient composite photocatalyst for hydrogen production and dye degradation. *ACS Omega* **2018**, *3*, 10980−10991.

(14) De, B.; Balamurugan, J.; Kim, N. H.; Lee, J. H. Enhanced electrochemical and photocatalytic performance of core-shell CuS@carbon quantum dots@carbon hollow nanospheres. *ACS Appl. Mater. Interfaces* **2017**, *9*, 2459−2468.

(15) Othong, J.; Boonmak, J.; Promarak, V.; Kielar, F.; Youngme, S. Sonochemical Synthesis of carbon dots/lanthanoid MOFs hybrids for white light-emitting diodes with high color rendering. *ACS Appl. Mater. Interfaces* **2019**, *11*, 44421−44429.

(16) Paulo-Mirasol, S.; Martinez-Ferrero, E.; Palomares, E. Direct white light emission from carbon nanodots (C-dots) in solution processed light emitting diodes. *Nanoscale* **2019**, *11*, 11315−11321.

(17) Guo, X.; Xu, D.; Yuan, H. M.; Luo, Q. Y.; Tang, S. Y.; Liu, L.; Wu, Y. Q. A novel fluorescent nanocellulosic hydrogel based on carbon dots for efficient adsorption and sensitive sensing in heavy metals. *J. Mater. Chem. A* **2019**, *7*, 27081−27088.

(18) Ding, H.; Yu, S. B.; Wei, J. S.; Xiong, H. M. Full-color light-emitting carbon dots with a surface-state-controlled luminescence mechanism. *ACS Nano* **2016**, *10*, 484−491.

(19) Zhang, X.; Jiang, M.; Niu, N.; Chen, Z.; Li, S.; Liu, S.; Li, J. Natural-product-derived carbon dots: from natural products to functional materials. *ChemSusChem* **2018**, *11*, 11−24.

(20) Zheng, X. T.; Ananthanarayanan, A.; Luo, K. Q.; Chen, P. Glowing graphene quantum dots and carbon dots: properties, syntheses, and biological applications. *Small* **2015**, *11*, 1620−1636.

(21) Teymourinia, H.; Salavati-Niasari, M.; Amiri, O.; Safardoust-Hojaghan, H. Synthesis of graphene quantum dots from corn powder and their application in reduce charge recombination and increase free charge carriers. *J. Mol. Liq.* **2017**, *242*, 447−455.

(22) Al-Douri, Y.; Badi, N.; Voon, C. H. Synthesis of carbon-based quantum dots from starch extracts: optical investigations. *Luminescence* **2018**, *33*, 260−266.

(23) Pacquiao, M. R.; de Luna, M. D. G.; Thongsai, N.; Kladsomboon, S.; Paoprasert, P. Highly fluorescent carbon dots from enokitake mushroom as multi-faceted optical nanomaterials for Cr^{6+} and VOC detection and imaging applications. *Appl. Surf. Sci.* **2018**, *453*, 192−203.

(24) Thongsai, N.; Jaiyong, P.; Kladsomboon, S.; In, I.; Paoprasert, P. Utilization of carbon dots from jackfruit for real-time sensing of acetone vapor and understanding the electronic and interfacial interactions using density functional theory. *Appl. Surf. Sci.* **2019**, *487*, 1233−1244.

(25) De, B.; Karak, N. A green and facile approach for the synthesis of water soluble fluorescent carbon dots from banana juice. *RSC Adv.* **2013**, *3*, 8286−8290.

(26) Bhamore, J. R.; Jha, S.; Singhal, R. K.; Park, T. J.; Kailasa, S. K. Facile green synthesis of carbon dots from pyrus pyrifolia fruit for assaying of Al^{3+} ion via chelation enhanced fluorescence mechanism. *J. Mol. Liq.* **2018**, *264*, 9−16.
(27) Thongsai, N.; Tanawannapong, N.; Praneerad, J.; Kladsomboon, S.; Jaiyong, P.; Paoprasert, P. Real-time detection of alcohol vapors and volatile organic compounds via optical electronic nose using carbon dots prepared from rice husk and density functional theory calculation. *Colloids Surf., A* **2019**, *560*, 278−287.
(28) Wang, W.; Wang, Z.; Liu, J.; Peng, Y.; Yu, X.; Wang, W.; Zhang, Z.; Sun, L. One-pot facile synthesis of graphene quantum dots from rice husks for Fe^{3+} sensing. *Ind. Eng. Chem. Res.* **2018**, *57*, 9144−9150.
(29) Zhan, J.; Peng, R. J.; Wei, S. X.; Chen, J.; Peng, X. H.; Xiao, B. Ethanol-precipitation-assisted highly efficient synthesis of nitrogen-doped carbon quantum dots from chitosan. *ACS Omega* **2019**, *4*, 22574−22580.
(30) Gao, X. X.; Zhou, X.; Ma, Y. F.; Qian, T.; Wang, C. P.; Chu, F. X. Facile and cost-effective preparation of carbon quantum dots for Fe^{3+} ion and ascorbic acid detection in living cells based on the "on-off-on" fluorescence principle. *Appl. Surf. Sci.* **2019**, *469*, 911−916.
(31) Cheng, C.; Xing, M.; Wu, Q. A universal facile synthesis of nitrogen and sulfur co-doped carbon dots from cellulose-based biowaste for fluorescent detection of Fe^{3+} ions and intracellular bioimaging. *Mater. Sci. Eng., C* **2019**, *99*, 611−619.
(32) Cheng, C.; Shi, Y.; Li, M.; Xing, M.; Wu, Q. Carbon quantum dots from carbonized walnut shells: structural evolution, fluorescence characteristics, and intracellular bioimaging. *Mater. Sci. Eng., C* **2017**, *79*, 473−480.
(33) Song, X.; Wang, H.; Zhang, R.; Yu, C.; Tan, M. Bio-distribution and interaction with dopamine of fluorescent nanodots from roasted chicken. *Food Funct.* **2018**, *9*, 6227−6235.
(34) Chiang, C. L.; Wu, M. T.; Dai, D. C.; Wen, Y. S.; Wang, J. K.; Chen, C. T. Red-emitting fluorenes as efficient emitting hosts for non-doped, organic red-light-emitting diodes. *Adv. Funct. Mater.* **2005**, *15*, 231−238.
(35) Yang, H. Y.; Liu, Y. L.; Guo, Z. Y.; Lei, B. F.; Zhuang, J. L.; Zhang, X. J.; Liu, Z. M.; Hu, C. F. Hydrophobic carbon dots with blue dispersed emission and red aggregation-induced emission. *Nat. Commun.* **2019**, *10*, No. 1789.
(36) Guo, R.; Li, T.; Shi, S. Aggregation-induced emission enhancement of carbon quantum dots and applications in light emitting devices. *J. Mater. Chem. C* **2019**, *7*, 5148−5154.
(37) Zhu, S.; Meng, Q.; Wang, L.; Zhang, J.; Song, Y.; Jin, H.; Zhang, K.; Sun, H.; Wang, H.; Yang, B. Highly Photoluminescent carbon dots for multicolor patterning, sensors, and bioimaging. *Angew. Chem., Int. Ed.* **2013**, *52*, 3953−3957.
(38) Chen, Y.; Zheng, M. T.; Xiao, Y.; Dong, H. W.; Zhang, H. R.; Zhuang, J. L.; Hu, H.; Lei, B. F.; Liu, Y. L. A self-quenching-resistant carbon-dot powder with tunable solid-state fluorescence and construction of dual-fluorescence morphologies for white light-emission. *Adv. Mater.* **2016**, *28*, 312−318.
(39) Peng, J.; Gao, W.; Gupta, B. K.; Liu, Z.; Romero-Aburto, R.; Ge, L.; Song, L.; Alemany, L. B.; Zhan, X.; Gao, G.; Vithayathil, S. A.; Kaipparettu, B. A.; Marti, A. A.; Hayashi, T.; Zhu, J.-J.; Ajayan, P. M. Graphene quantum dots derived from carbon fibers. *Nano Lett.* **2012**, *12*, 844−849.
(40) Hu, C. F.; Liu, Y. L.; Yang, Y. H.; Cui, J. H.; Huang, Z. R.; Wang, Y. L.; Yang, L. F.; Wang, H. B.; Xiao, Y.; Rong, J. H. One-step preparation of nitrogen-doped graphene quantum dots from oxidized debris of graphene oxide. *J. Mater. Chem. B* **2013**, *1*, 39−42.
(41) Long, P.; Feng, Y.; Li, Y.; Cao, C.; Li, S.; An, H.; Qin, C.; Han, J.; Feng, W. Solid-state fluorescence of fluorine-modified carbon nanodots aggregates triggered by poly(ethylene glycol). *ACS Appl. Mater. Interfaces* **2017**, *9*, 37981−37990.
(42) Wang, Z.; Yuan, F.; Li, X.; Li, Y.; Zhong, H.; Fan, L.; Yang, S. 53% efficient red emissive carbon quantum dots for high color rendering and stable warm white-light-emitting diodes. *Adv. Mater.* **2017**, *29*, No. 1702910.
(43) Bi, Z.; Li, T.; Su, H.; Ni, Y.; Yan, L. Transparent wood film incorporating carbon dots as encapsulating material for white light-emitting diodes. *ACS Sustainable Chem. Eng.* **2018**, *6*, 9314−9323.
(44) Shen, J.; Shang, S.; Chen, X.; Wang, D.; Cai, Y. Facile synthesis of fluorescence carbon dots from sweet potato for Fe^{3+} sensing and cell imaging. *Mater. Sci. Eng., C* **2017**, *76*, 856−864.
(45) He, T.; Niu, N.; Chen, Z.; Li, S.; Liu, S.; Li, J. Novel quercetin aggregation-induced emission luminogen (AIEgen) with excited-state intramolecular proton transfer for in vivo bioimaging. *Adv. Funct. Mater.* **2018**, *28*, No. 1706196.
(46) Cosnier, S.; Le Goff, A.; Holzinger, M. Towards glucose biofuel cells implanted in human body for powering artificial organs: Review. *Electrochem. Commun.* **2014**, *38*, 19−23.
(47) Ananthanarayanan, A.; Wang, X. W.; Routh, P.; Sana, B.; Lim, S.; Kim, D. H.; Lim, K. H.; Li, J.; Chen, P. Facile synthesis of graphene quantum dots from 3d graphene and their application for Fe^{3+} sensing. *Adv. Funct. Mater.* **2014**, *24*, 3021−3026.
(48) Chandra, S.; Laha, D.; Pramanik, A.; Ray Chowdhuri, A.; Karmakar, P.; Sahu, S. K. Synthesis of highly fluorescent nitrogen and phosphorus doped carbon dots for the detection of Fe^{3+} ions in cancer cells. *Luminescence* **2016**, *31*, 81−87.

https://dx.doi.org/10.1021/acsomega.0c01527
ACS Omega 2020, 5, 11842−11848